

Supplementary Materials

Increasing the Efficiency of Optimized V-SBA-15 Catalysts in the Selective Oxidation of Methane to Formaldehyde by Artificial Neural Network Modelling

Benny Kunkel^{1,*}, Anke Kabelitz², Ana Guilherme Buzanich² and Sebastian Wohlrab^{1,*}

¹ Leibniz-Institut für Katalyse e.V. an der Universität Rostock, Albert-Einstein-Str. 29a, 18059 Rostock, Germany

² Bundesanstalt für Materialforschung und -Prüfung (BAM), Richard-Willstätter-Straße 11, 12489 Berlin, Germany; Anke.Kabelitz@bam.de (A.K.); Ana.Buzanich@bam.de (A.G.B.)

* Correspondence: Benny.Kunkel@catalysis.de (B.K.); Sebastian.Wohlrab@catalysis.de (S.W.)

Formulae for the calculation of catalytic parameters:

$$X_{CH_4} = \sum_i Y_i \quad (S1)$$

$$S_i = \frac{Y_i}{X_{CH_4}} \cdot 100\% \quad (S2)$$

$$Y_i = \frac{v_i(c_i^P - c_i^E)}{c_{CH_4}^E} \cdot 100\% \quad (S3)$$

$$STY_{CH_2O} = \frac{1 \cdot 10^{-5} \cdot Y_{CH_2O} \cdot F_{CH_4} \cdot v_{CH_4}^{-1} \cdot M_{CH_2O}}{m_{cat}} \quad (S4)$$

Conversion of methane – X_{CH_4} [%]

Selectivity towards product i – S_i [%]

Yield of product i – Y_i [%]

Space-time yield of formaldehyde – STY_{CH_2O} [kg $_{CH_2O}$ ·kg $_{cat}^{-1}$ ·h $^{-1}$]

Stoichiometric number of component i – v_i [-]

Concentration of component i in the product/educt gas stream – c_i^P/c_i^E [%]

Flow of methane – F_{CH_4} [L·h $^{-1}$]

Molar volume of methane – v_{CH_4} [L·mol $^{-1}$]

Molar mass of formaldehyde – M_{CH_2O} [g·mol $^{-1}$]

Catalyst mass – m_{cat} [kg]

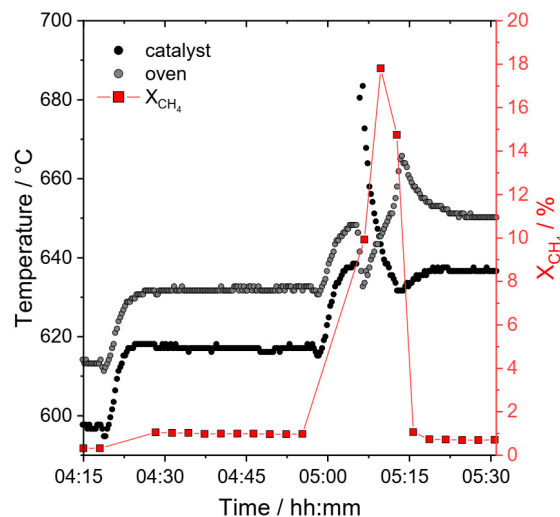


Figure S1. Temperature at the catalyst bed and oven and methane conversion over time. Reaction conditions: 25 mg, GHSV = 960,000 L·kg $^{-1}$ ·h $^{-1}$, CH $_4$:O $_2$ 8:2, 20% H $_2$ O.

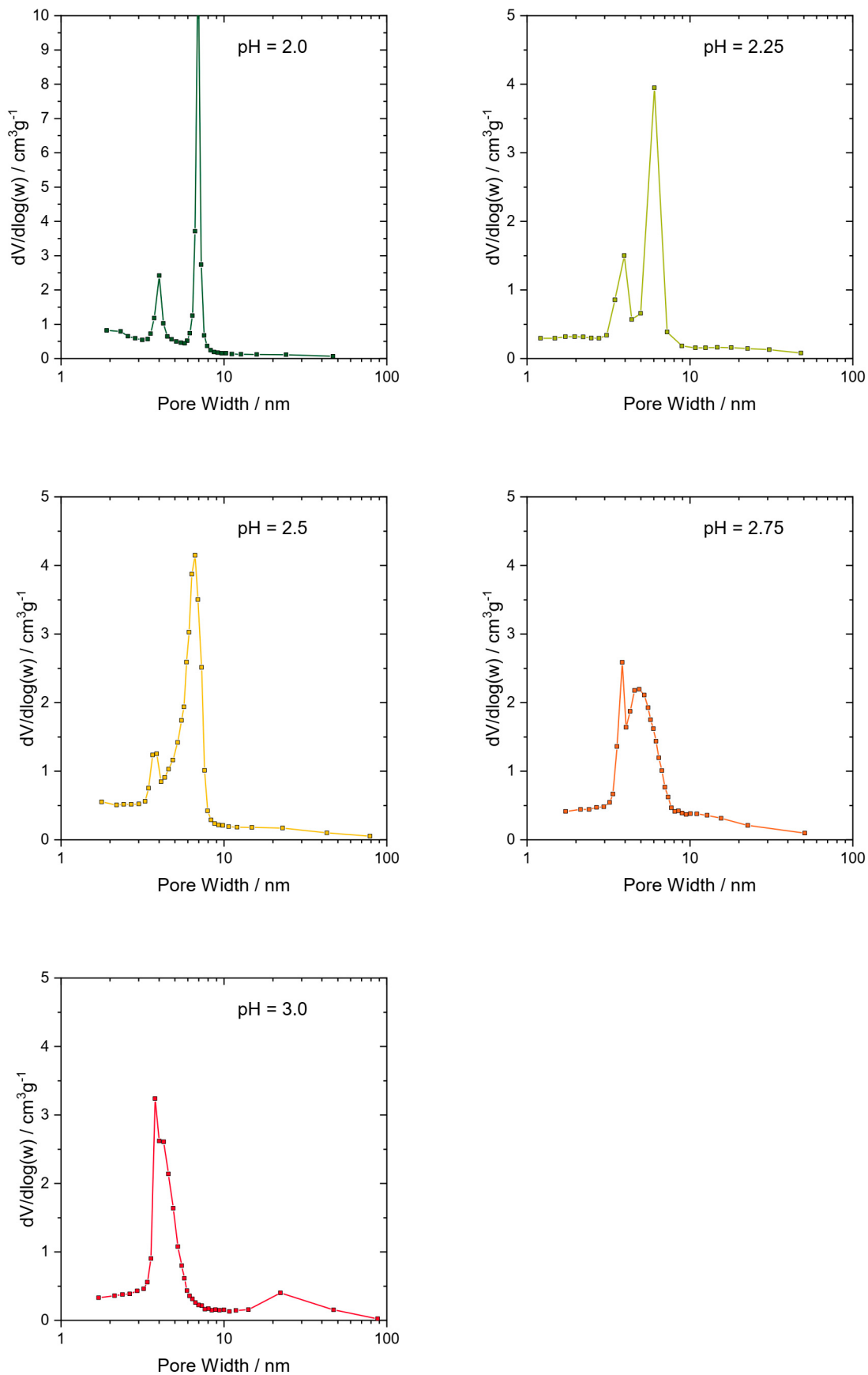


Figure S2. Pore size distribution of V-SBA-15 catalysts from BJH analyses.

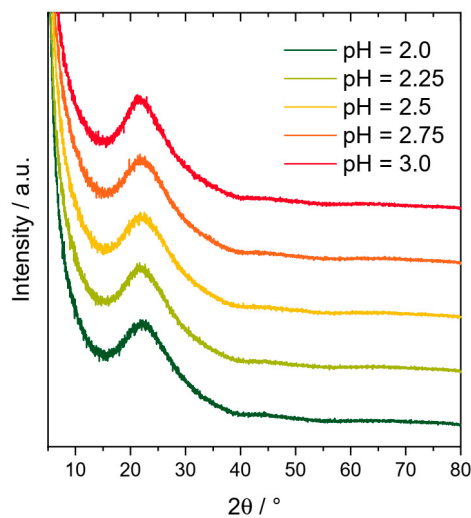


Figure S3. Wide-angle X-ray diffraction patterns of V-SBA-15 catalysts.

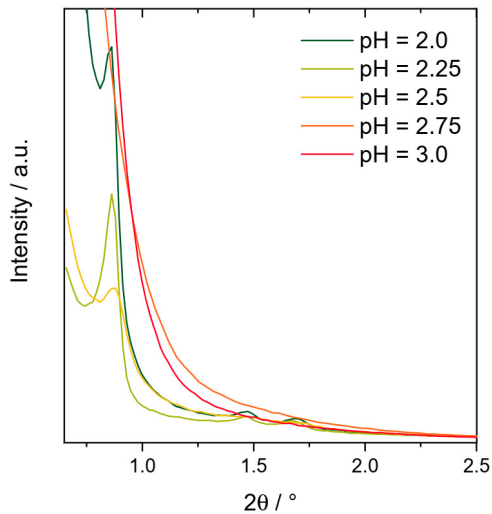


Figure S4. Small-angle X-ray diffraction patterns of V-SBA-15 catalysts.

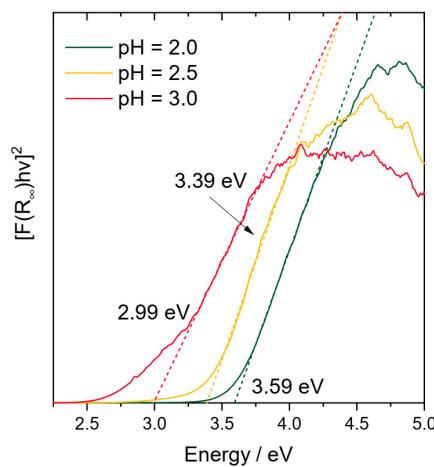


Figure S5. Tauc plots for UV-vis spectra of V-SBA-15(2.0), V-SBA-15(2.5) and V-SBA-15(3.0).

Table S1. Position ($\lambda_{\text{C}x}$) and ratio of the areas (A_x) of the deconvoluted gaussians for UV-vis spectra of V-SBA-15(2.0), V-SBA-15(2.5) and V-SBA-15(3.0).

	V-SBA-15(2.0)	V-SBA-15(2.5)	V-SBA-15(3.0)
$\lambda_{\text{C}1} / \text{nm}; A_1 / \%$	244; 24	247; 22	243; 16
$\lambda_{\text{C}2} / \text{nm}; A_2 / \%$	291; 67	303; 60	301; 42
$\lambda_{\text{C}3} / \text{nm}; A_3 / \%$	374; 9	387; 18	387; 42

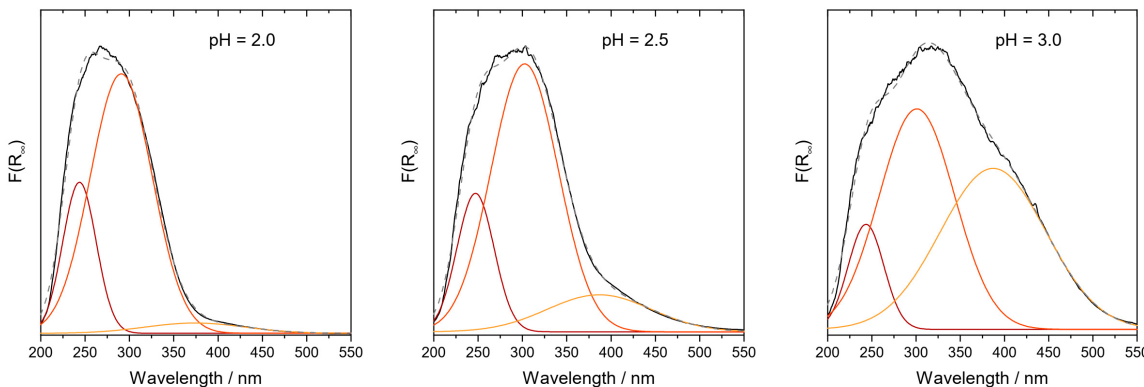


Figure S6. Deconvoluted UV-vis spectra of V-SBA-15(2.0), V-SBA-15(2.5) and V-SBA-15(3.0). Black – experimental spectrum; Grey dashed – sum of gaussians; Red/Orange/Yellow – gaussians.

Table S2. Pre-edge peak position of V-SBA-15 materials and reference compounds.

Material	Pre-edge peak position / eV
NH ₄ VO ₃	5468.46
V-SBA-15 (2.0)	5469.49
V-SBA-15 (2.25)	5469.49
V-SBA-15 (2.5)	5469.49
V-SBA-15 (2.75)	5469.49
V-SBA-15 (3.0)	5469.49
V ₂ O ₅	5469.50

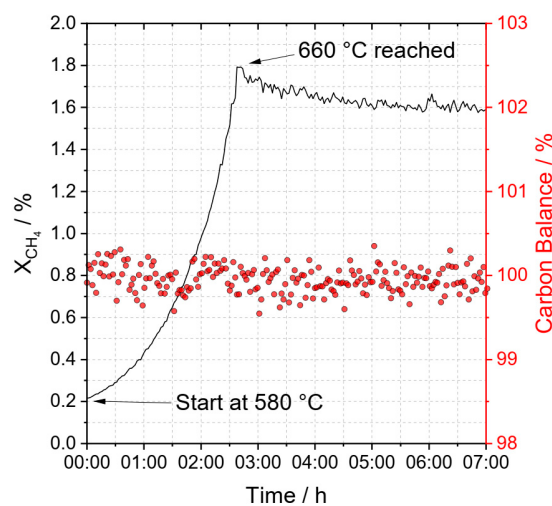


Figure S7. Methane conversion (black) and carbon balance (red) over time while heating up from 580 to 660 °C (heating rate 2 K·min⁻¹) and maintaining 660 °C. The carbon balance is calculated as ratio of carbon concentration in the product gas measured at the respective temperature to the sum of methane concentration measured at 200 °C. Reaction conditions: V-SBA-15(2.5), 720,000 L·kg⁻¹·h⁻¹, 90% CH₄ and 10% O₂.

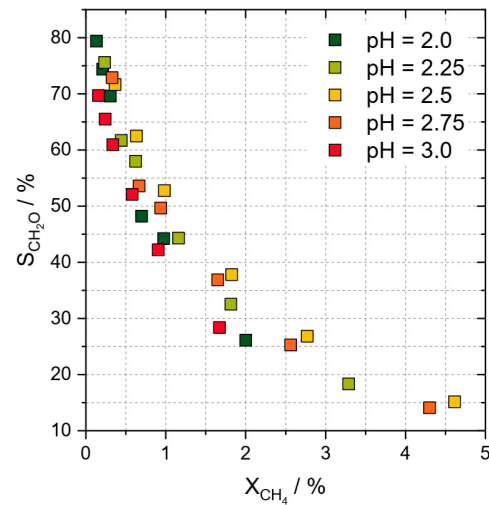


Figure S8. Formaldehyde selectivity vs. methane conversion plot at 620 °C (25 mg, GHSV = 720,000–120,000 L·kg⁻¹·h⁻¹, CH₄:O₂ 9:1).

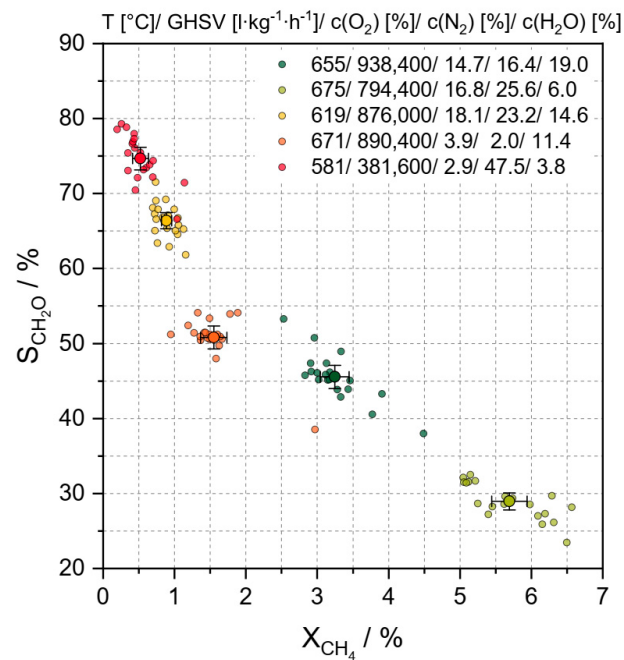


Figure S9. Output of the 20 single neural networks at five different conditions. The big markers indicate the average value and the whiskers represent 95% confidence interval.

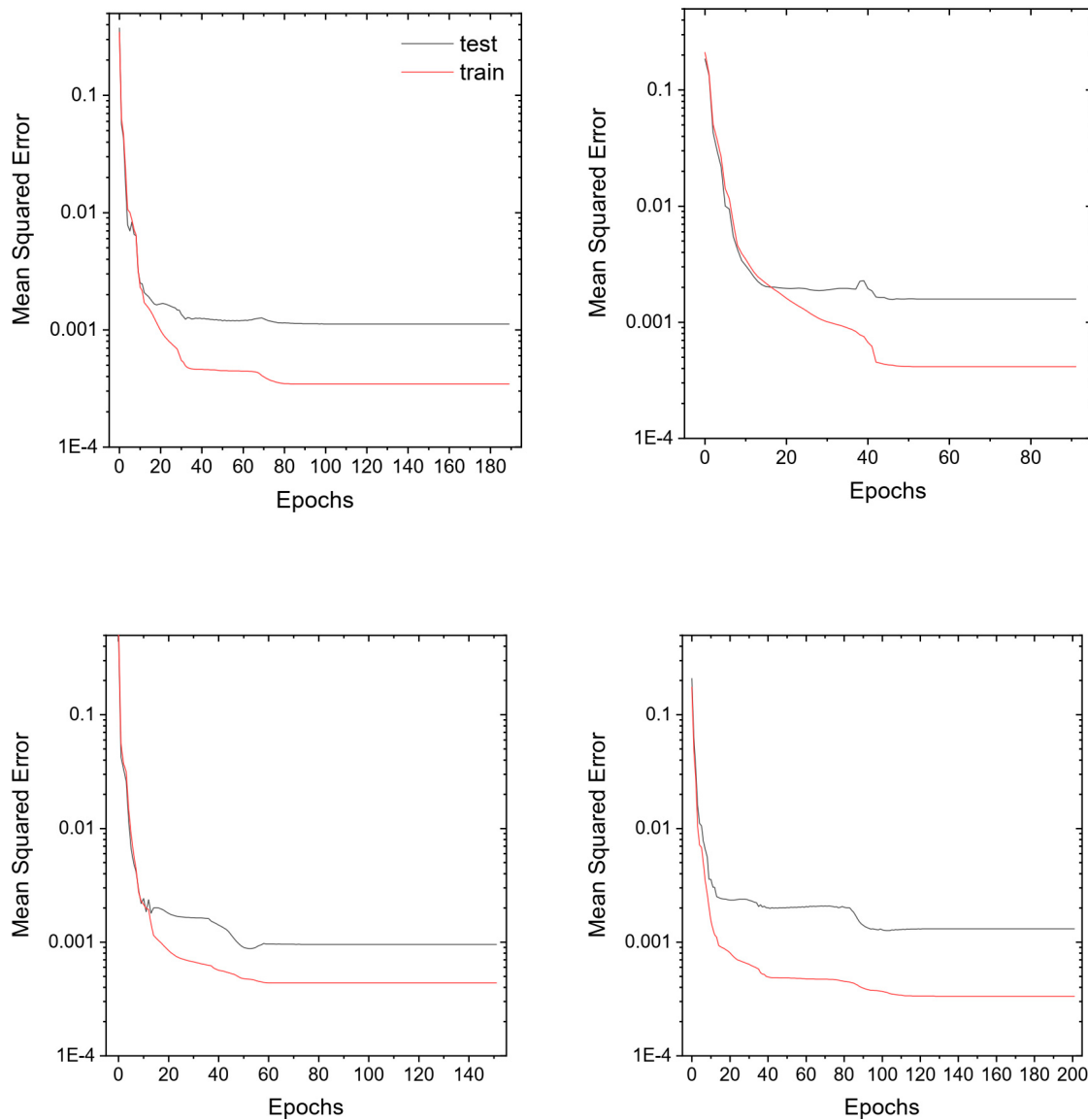


Figure S10. Performance of 5-10-2-2 neural networks in combination with BR learning on training and test data at different stages of the learning process. Data were randomly divided into training (75%) and test set (25%).

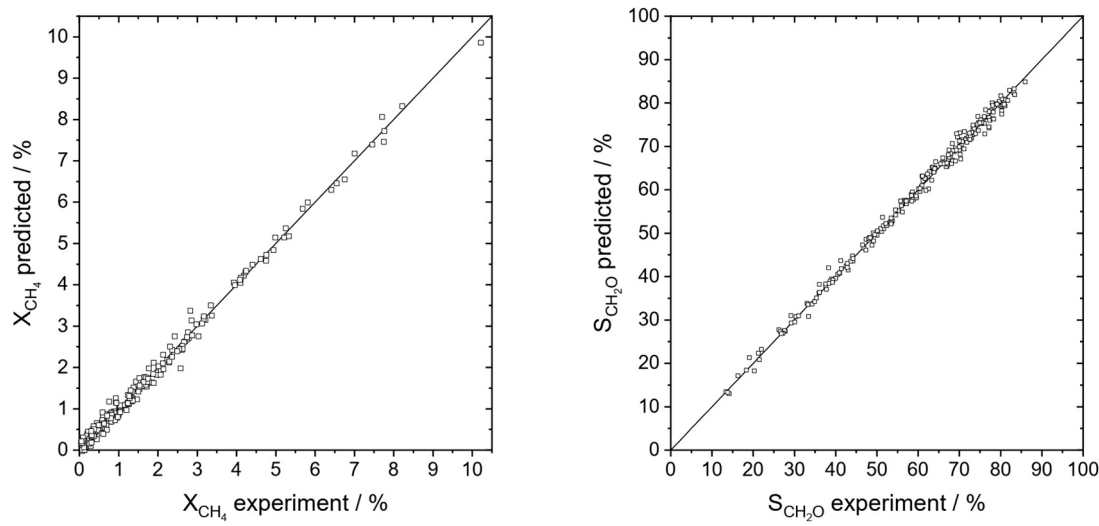


Figure S11. Correlation of predicted and experimental methane conversion and formaldehyde selectivity. Identity function is shown for comparison.

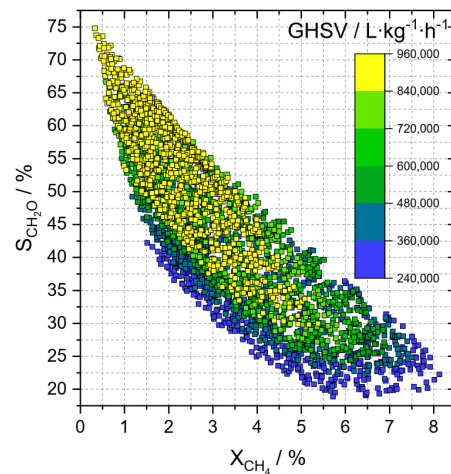


Figure S12. Predicted selectivity and conversion at 660 °C over the whole input range. Markers are coloured by GHSV.

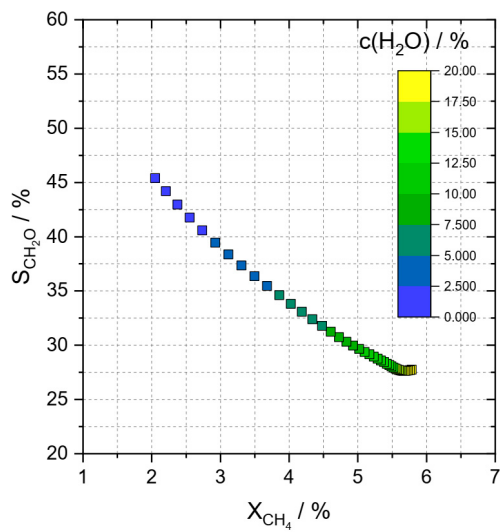


Figure S13. Predicted selectivity and conversion at 660 °C, 720,000 L·kg⁻¹·h⁻¹, 15% O₂ and 20% (N₂ + H₂O).

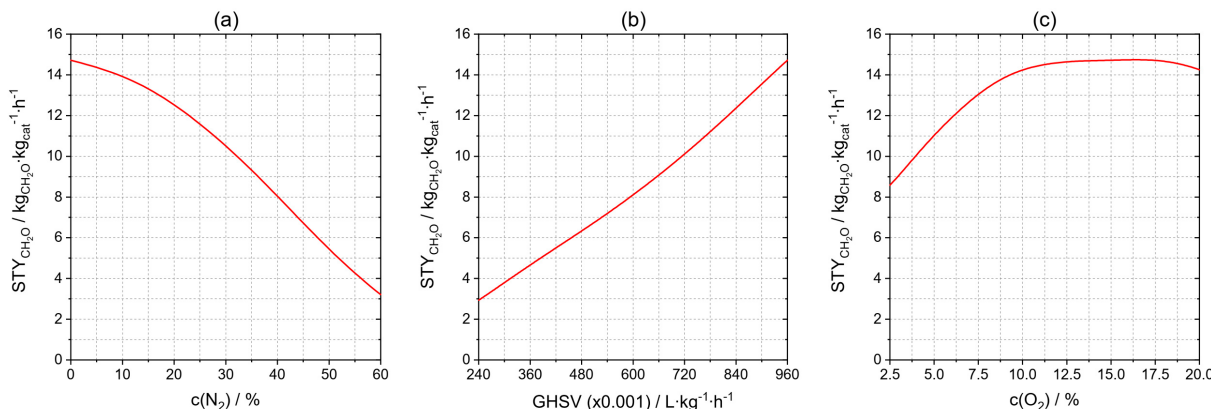


Figure S14. Predicted space-time yield at 680 °C, 960,000 L·kg⁻¹·h⁻¹, 15% O₂ and 20% H₂O with varying nitrogen dilution (a), GHSV (b) or oxygen concentration (c).

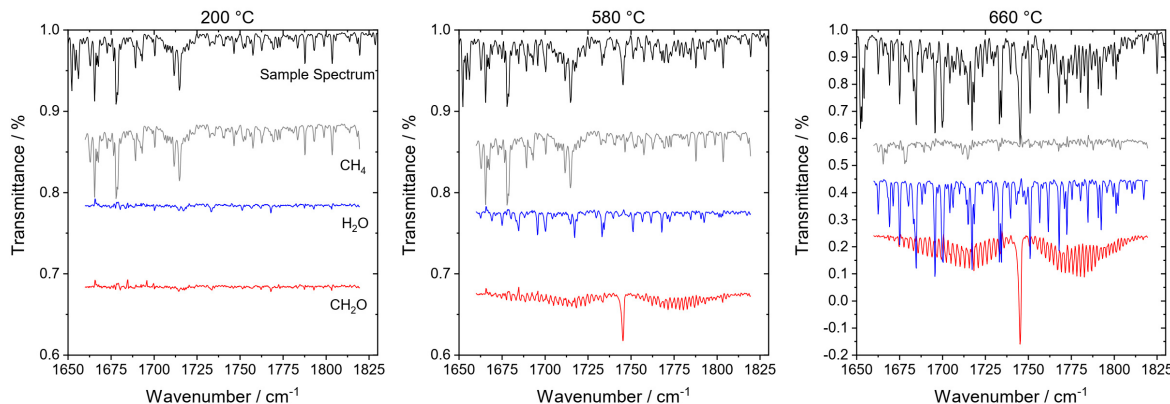


Figure S15. IR spectra of product gas obtained at different temperatures at 720,000 L·kg⁻¹·h⁻¹ and 10% O₂. Shown are the measured sample spectrum (black) as well as the fitted contributions of CH₄ (grey), H₂O (blue) and CH₂O (red).

Table S3. Training data for the neural network.

T / °C	GHSV / L·kg ⁻¹ ·h ⁻¹	c(O ₂) ^a / %	c(N ₂) ^b / %	c(H ₂ O) ^b / %	X _{CH₄} / %	S _{CH₂O} / %
580	240,000	5	20	2.5	0.54968	70.19706
600	240,000	5	20	2.5	1.02036	61.82707
620	240,000	5	20	2.5	1.62472	53.22689
640	240,000	5	20	2.5	2.24334	42.54023
660	240,000	5	20	2.5	2.7904	33.09023
680	240,000	5	20	2.5	3.21052	26.24107
580	240,000	15	20	10	0.65282	68.14057
600	240,000	15	20	10	1.38387	51.35819
620	240,000	15	20	10	2.76549	39.99169
640	240,000	15	20	10	4.62132	26.83839
660	240,000	15	20	10	6.55504	18.34626
680	240,000	15	20	10	7.7072	14.18006
580	240,000	20	40	5	0.62364	76.15251
600	240,000	20	40	5	1.33417	60.95622
620	240,000	20	40	5	2.61484	51.18517
640	240,000	20	40	5	4.4075	35.97764
660	240,000	20	40	5	7.00916	22.05047
680	240,000	20	40	5	10.21701	13.40938
580	240,000	15	60	0	0.42286	63.40421
600	240,000	15	60	0	0.88599	56.30939
620	240,000	15	60	0	1.56382	48.85086
640	240,000	15	60	0	2.36487	37.61487
660	240,000	15	60	0	3.34609	29.24018
680	240,000	15	60	0	4.76277	21.25642
580	480,000	5	60	5	0.34127	75.73964
600	480,000	5	60	5	0.65109	70.3295
620	480,000	5	60	5	1.01026	63.63907
640	480,000	5	60	5	1.35432	56.73608
660	480,000	5	60	5	1.6588	50.03626
680	480,000	5	60	5	1.89538	43.08058
580	480,000	15	20	5	0.35438	77.88303
600	480,000	15	20	5	0.79819	68.31164
620	480,000	15	20	5	1.66811	59.18766
640	480,000	15	20	5	2.98266	42.83965
660	480,000	15	20	5	5.21696	27.77735
680	480,000	15	20	5	7.46041	16.32157
580	240,000	2.5	0	15	0.47206	71.70366
600	240,000	2.5	0	15	1.00559	67.04664
620	240,000	2.5	0	15	1.47403	56.8505
640	240,000	2.5	0	15	1.81211	47.38603
660	240,000	2.5	0	15	2.01195	40.48819
680	240,000	2.5	0	15	2.13524	34.30984
580	240,000	10	40	15	0.20765	75.34681
600	240,000	10	40	15	0.71948	70.24263
620	240,000	10	40	15	1.44713	56.08164
640	240,000	10	40	15	2.43174	44.22532
660	240,000	10	40	15	4.1066	29.18206
680	240,000	10	40	15	5.25429	19.12338
580	240,000	20	40	0	0.35232	61.23143
600	240,000	20	40	0	0.82224	53.79426

620	240,000	20	40	0	1.52826	41.36866
640	240,000	20	40	0	2.85911	30.41555
660	240,000	20	40	0	4.98702	21.5088
680	240,000	20	40	0	7.74955	13.81935
580	240,000	5	40	2.5	0.60383	77.21426
600	240,000	5	40	2.5	1.05714	64.24443
620	240,000	5	40	2.5	1.71716	57.19379
640	240,000	5	40	2.5	2.28593	46.90609
660	240,000	5	40	2.5	2.74108	37.77518
680	240,000	5	40	2.5	3.16406	30.06403
580	960,000	10	20	20	0.04426	69.56067
600	960,000	10	20	20	0.26728	70.53118
620	960,000	10	20	20	0.7519	68.36957
640	960,000	10	20	20	1.58966	62.55887
660	960,000	10	20	20	2.69923	49.12469
680	960,000	10	20	20	3.93543	36.04715
580	480,000	5	60	2.5	0.38821	77.00651
600	480,000	5	60	2.5	0.68795	72.93438
620	480,000	5	60	2.5	1.04515	66.80394
640	480,000	5	60	2.5	1.36035	55.79572
660	480,000	5	60	2.5	1.70189	48.27643
680	480,000	5	60	2.5	2.08	40.99325
580	720,000	5	0	0	0.08026	85.95162
600	720,000	5	0	0	0.16957	83.17699
620	720,000	5	0	0	0.29908	80.27844
640	720,000	5	0	0	0.45749	70.66352
660	720,000	5	0	0	0.68615	61.15611
680	720,000	5	0	0	1.15863	51.65804
580	720,000	5	60	0	0.10968	79.73874
600	720,000	5	60	0	0.17585	77.6854
620	720,000	5	60	0	0.26906	74.70115
640	720,000	5	60	0	0.38363	71.61476
660	720,000	5	60	0	0.52816	65.9006
680	720,000	5	60	0	0.76638	58.39986
580	480,000	20	20	0	0.09497	77.96401
600	480,000	20	20	0	0.23266	75.40855
620	480,000	20	20	0	0.53185	70.36555
640	480,000	20	20	0	1.03286	55.19969
660	480,000	20	20	0	2.58076	38.25356
680	480,000	20	20	0	2.82836	33.43277
580	960,000	10	40	0	0.05699	82.20959
600	960,000	10	40	0	0.12625	80.41804
620	960,000	10	40	0	0.24549	77.21901
640	960,000	10	40	0	0.39302	73.80242
660	960,000	10	40	0	0.60609	67.181
680	960,000	10	40	0	0.93185	54.55336
580	720,000	2.5	20	0	0.14465	78.10866
600	720,000	2.5	20	0	0.22697	75.48013
620	720,000	2.5	20	0	0.32689	70.72512
640	720,000	2.5	20	0	0.45184	63.50452
660	720,000	2.5	20	0	0.59178	55.95905
680	720,000	2.5	20	0	0.76444	48.10208

580	720,000	2.5	60	0	0.09464	78.98856
600	720,000	2.5	60	0	0.16256	78.21591
620	720,000	2.5	60	0	0.24921	76.05721
640	720,000	2.5	60	0	0.34194	72.62123
660	720,000	2.5	60	0	0.44657	67.37243
680	720,000	2.5	60	0	0.58838	60.80283
580	960,000	2.5	40	0	0.0784	80.08721
600	960,000	2.5	40	0	0.13428	81.2447
620	960,000	2.5	40	0	0.20912	79.9455
640	960,000	2.5	40	0	0.29164	77.15843
660	960,000	2.5	40	0	0.39197	72.17619
680	960,000	2.5	40	0	0.54252	65.51004
580	480,000	20	60	10	0.2185	76.35393
600	480,000	20	60	10	0.89883	73.32653
620	480,000	20	60	10	1.75972	63.95817
640	480,000	20	60	10	2.87576	54.61955
660	480,000	20	60	10	4.18625	43.68026
680	480,000	20	60	10	5.68692	33.29887
580	240,000	2.5	0	5	0.47694	72.57979
600	240,000	2.5	0	5	0.89881	66.28549
620	240,000	2.5	0	5	1.23854	57.45002
640	240,000	2.5	0	5	1.53153	48.07343
660	240,000	2.5	0	5	1.69773	40.86562
680	240,000	2.5	0	5	1.77401	34.95417
580	960,000	2.5	0	2.5	0.13875	83.30174
600	960,000	2.5	0	2.5	0.29057	81.79021
620	960,000	2.5	0	2.5	0.4462	75.16166
640	960,000	2.5	0	2.5	0.70399	70.37406
660	960,000	2.5	0	2.5	0.95539	60.96761
680	960,000	2.5	0	2.5	1.23616	50.93288
580	480,000	2.5	0	20	0.18785	72.68632
600	480,000	2.5	0	20	0.46056	70.04231
620	480,000	2.5	0	20	0.81185	62.7882
640	480,000	2.5	0	20	1.33753	58.90944
660	480,000	2.5	0	20	1.7428	50.1269
680	480,000	2.5	0	20	2.01736	42.86687
580	480,000	5	20	2.5	0.27504	80.35802
600	480,000	5	20	2.5	0.49831	73.31007
620	480,000	5	20	2.5	0.82757	66.03315
640	480,000	5	20	2.5	1.30716	59.63009
660	480,000	5	20	2.5	1.7547	49.17821
680	480,000	5	20	2.5	2.28977	39.04641
580	720,000	5	20	20	0.06351	70.08682
600	720,000	5	20	20	0.34882	72.32361
620	720,000	5	20	20	0.73591	68.78576
640	720,000	5	20	20	1.26955	63.83378
660	720,000	5	20	20	1.85871	58.49169
680	720,000	5	20	20	2.36411	49.53248
580	960,000	20	20	5	0.0939	80.58218
600	960,000	20	20	5	0.2945	77.38163
620	960,000	20	20	5	0.62193	69.98584
640	960,000	20	20	5	1.23617	58.62883

660	960,000	20	20	5	2.66663	44.0993
580	960,000	2.5	0	15	0.09798	74.42529
600	960,000	2.5	0	15	0.2627	73.94932
620	960,000	2.5	0	15	0.47228	69.07511
640	960,000	2.5	0	15	0.73219	64.168
660	960,000	2.5	0	15	1.04394	60.47582
680	960,000	2.5	0	15	1.31243	53.46242
580	960,000	15	20	10	0.07785	74.48187
600	960,000	15	20	10	0.31328	73.61588
620	960,000	15	20	10	0.75025	68.47372
640	960,000	15	20	10	1.63401	61.91072
660	960,000	15	20	10	3.17345	47.30749
670	960,000	15	20	10	4.23021	37.61956
580	480,000	10	60	5	0.30032	81.09584
600	480,000	10	60	5	0.8182	77.16632
620	480,000	10	60	5	1.33835	67.84477
640	480,000	10	60	5	1.9728	58.77809
660	480,000	10	60	5	2.62494	48.40187
680	480,000	10	60	5	3.3741	38.69068
580	960,000	10	0	10	0.13032	75.40735
600	960,000	10	0	10	0.37198	71.80551
620	960,000	10	0	10	0.7554	61.27104
640	960,000	10	0	10	1.53782	51.63638
660	960,000	10	0	10	2.7419	39.40862
680	960,000	10	0	10	4.1179	27.62165
580	720,000	15	20	5	0.26017	79.16451
600	720,000	15	20	5	0.57012	73.33196
620	720,000	15	20	5	1.20722	67.00884
640	720,000	15	20	5	2.13033	52.32374
660	720,000	15	20	5	3.95843	35.37943
670	720,000	15	20	5	5.33443	26.52983
580	720,000	20	20	20	0.08367	73.03287
600	720,000	20	20	20	0.35042	69.26278
620	720,000	20	20	20	0.93421	61.66312
640	720,000	20	20	20	2.31289	53.55989
660	720,000	20	20	20	4.94285	38.40637
670	720,000	20	20	20	6.41788	31.03182
580	960,000	10	40	2.5	0.12668	83.43866
600	960,000	10	40	2.5	0.31561	80.86242
620	960,000	10	40	2.5	0.6103	78.14818
640	960,000	10	40	2.5	0.91476	70.05516
660	960,000	10	40	2.5	1.36334	61.12742
680	960,000	10	40	2.5	2.07349	53.47923
580	240,000	15	40	15	0.63281	72.63995
600	240,000	15	40	15	1.50421	62.26363
620	240,000	15	40	15	3.03582	52.42996
640	240,000	15	40	15	4.75216	39.25382
660	240,000	15	40	15	6.75668	27.20579
680	240,000	15	40	15	8.22181	20.25856
580	720,000	20	60	15	0.09721	80.29377
600	720,000	20	60	15	0.4979	71.20908
620	720,000	20	60	15	1.2404	67.56691

640	720,000	20	60	15	2.13985	60.08599
660	720,000	20	60	15	3.12515	52.1463
680	720,000	20	60	15	4.2462	44.21365
580	240,000	20	60	20	0.36344	74.9785
600	240,000	20	60	20	1.28344	67.90845
620	240,000	20	60	20	2.6325	59.54416
640	240,000	20	60	20	4.08906	46.51509
660	240,000	20	60	20	5.81344	36.08289
680	240,000	20	60	20	7.76703	26.84423
580	960,000	20	0	20	0.04711	69.37535
600	960,000	20	0	20	0.31768	71.12844
620	960,000	20	0	20	0.98208	63.33159
580	960,000	15	0	20	0.10444	72.56513
600	960,000	15	0	20	0.37931	69.04459
620	960,000	15	0	20	0.9467	57.13113
640	960,000	15	0	20	2.54853	41.26486
580	960,000	20	20	10	0.07503	76.08092
600	960,000	20	20	10	0.32121	74.61641
620	960,000	20	20	10	0.80717	67.31772
640	960,000	20	20	10	1.8981	58.43734
580	720,000	10	60	20	0.06153	78.32957
600	720,000	10	60	20	0.30389	72.46344
620	720,000	10	60	20	0.71037	67.50521
640	720,000	10	60	20	1.27236	64.01048
660	720,000	10	60	20	1.88486	60.49665
680	720,000	10	60	20	2.49153	56.2183

a – concentration relative to methane; b – absolute concentration.